Research Square

Preprints are preliminary reports that have not undergone peer review.
They should not be considered conclusive, used to inform clinical practice,
or referenced by the media as validated information.

Concurrent Noonan Syndrome and Sanjad-Sakati Syndrome in a Newborn: First Genetically Confirmed Dual Diagnosis

Maryam Aburezq
maryam.burezq@gmail.com

Farwaniya Hospital
Doaa Ibrahim
Kuwait Medical Genetics Center
Laila Bastaki
Kuwait Medical Genetics Center
Aditya Raina
Maternaty Hospital
Yasmeen Fathy
Maternaty Hospital
Mariam Ayed
Maternaty Hospital

Research Article

Keywords: Noonan syndrome, Sanjad-Sakati syndrome, blended phenotype, RIT1, TBCE, dual molecular diagnosis

Posted Date: August 25th, 2026

DOI: https://doi.org/10.21203/rs.3.rs-10518207/v1

License: This work is licensed under a Creative Commons Attribution 4.0 International License. Read Full License

Additional Declarations: No competing interests reported.

Abstract

Purpose: To describe the first genetically confirmed coexistence of Noonan syndrome and Sanjad-Sakati syndrome in a newborn and to highlight the diagnostic challenges posed by overlapping and blended phenotypes.

Methods: A case report of an infant with dual molecular diagnoses of Noonan syndrome and Sanjad-Sakati syndrome based on clinical, biochemical, radiological, and genomic findings.

Results: A male infant born at 36 weeks' gestation with severe intrauterine growth restriction, non-immune hydrops fetalis, and phenotypic features suggestive of Noonan syndrome. His clinical course was complicated by bilateral pleural effusions, congenital heart disease, severe gastroesophageal reflux with aspiration pneumonia, renal dysplasia with nephrocalcinosis, congenital hypothyroidism, hypoparathyroidism with hypocalcemic seizures, persistent thrombocytopenia, and recurrent multidrug-resistant sepsis. Whole-exome sequencing identified a heterozygous pathogenic *RIT1* variant, confirming Noonan syndrome, and a homozygous pathogenic *TBCE* variant, confirming Sanjad-Sakati syndrome; heterozygous *CYP21A2* and *POLG* carrier variants were also detected. The infant died at 142 days of life from refractory septic shock and multiorgan failure.

Conclusions: This first genetically confirmed coexistence of Noonan syndrome and Sanjad-Sakati syndrome highlights the diagnostic challenges of blended phenotypes and emphasizes the value of early genomic testing, multidisciplinary care, and genetic counseling.

BACKGROUND

Noonan syndrome (NS) [OMIM: 163950] is a RASopathy caused by dysregulation of the RAS-mitogen-activated protein kinase (RAS-MAPK) pathway, affecting approximately 1 in 1,000–2,500 individuals worldwide without sex or ethnic predilection (Zenker et al. 2022; Sharma et al. 2025). NS is primarily inherited in an autosomal dominant (AD) manner; however, *de novo* and, rarely, autosomal recessive (AR) cases have been reported (Roberts et al. 2013; Aoki et al. 2016; Sharma et al. 2025). It is a clinically heterogeneous disorder characterized by craniofacial dysmorphism, congenital heart disease (CHD), lymphatic dysplasia, and multiorgan involvement (Roberts 1993; Roberts et al. 2013; Carcavilla et al. 2020; Sharma et al. 2025). Characteristic craniofacial features, most prominent during childhood, include hypertelorism, down-slanting palpebral fissures, epicanthic folds, low-set posteriorly rotated ears with fleshy helices (Roberts 1993; Sharma et al. 2025), webbed neck, and a low posterior hairline (Roberts et al. 2013; Sharma et al. 2025). CHD occurs in 70–80% of cases (Roberts 1993), most commonly pulmonary valve stenosis, hypertrophic cardiomyopathy, septal defects, and electrocardiographic abnormalities in the absence of structural heart disease (Roberts 1993; Roberts et al. 2013; Carcavilla et al. 2020). Additional manifestations include cryptorchidism (60–80%), renal anomalies (10%) (Roberts et al. 2013), autoimmune thyroiditis, bleeding diathesis, and an increased risk of hematologic and solid malignancies (Carcavilla et al. 2020). Skeletal manifestations include a broad chest with widely spaced nipples, pectus and spinal deformities (Carcavilla et al. 2020). Postnatal growth deceleration results in adulthood short stature despite normal birth length (Roberts 1993; Carcavilla et al. 2020; Sharma et al. 2025). Transient neonatal feeding difficulties requiring temporary nasogastric support occur in approximately 25% of cases (Carcavilla et al. 2020), while developmental delay (DD) and intellectual disability (ID) are reported in a similar proportion (Roberts 1993), More than 20 causative genes have been identified (Carcavilla et al. 2020), with *PTPN11* accounting for approximately half of molecularly confirmed cases (Roberts 1993; Saint-Laurent et al. 2023). *RIT1* [NM_006912.6] variants account for 5–10% of cases and are frequently associated with severe neonatal phenotypes (Aoki et al. 2013). Molecular confirmation is established by targeted gene panels or comprehensive genomic sequencing (Roberts 1993), although 20–30% of clinically diagnosed cases remain molecularly unresolved (Saint-Laurent et al. 2023).

Sanjad-Sakati syndrome (SSS) [OMIM: 241410], also known as hypoparathyroidism-retardation-dysmorphism syndrome, is a rare AR disorder characterized by distinctive facial dysmorphism, congenital hypoparathyroidism, intrauterine growth restriction (IUGR), DD, and variable ID (Elhassanien and Alghiaty 2013; Benchaib et al. 2024). It is predominantly reported in Middle Eastern and North African populations, with an estimated incidence in Saudi Arabia of 1:40,000-600,000 live births (Benchaib et al. 2024). Affected neonates typically present with early-onset hypocalcemic seizures secondary to congenital hypoparathyroidism or non-parathyroid-related causes (Benchaib et al. 2024). Characteristic craniofacial features include microcephaly, a prominent forehead, a long narrow face, micrognathia, a beaked nose, deep-set eyes, thin lips, low-set floppy ears, and dental anomalies (Elhassanien and Alghiaty 2013; Benchaib et al. 2024). These features are often associated with severe prenatal and postnatal growth retardation as well as infantile feeding difficulty (David et al. 2021; Benchaib et al. 2024). Moreover, hypothyroidism is reported in up to 36% of cases, some

of which were congenital hypothyroidism and others autoimmune thyroiditis (David et al. 2021; Benchaib et al. 2024). Diagnosis is confirmed by biallelic pathogenic variants in *TBCE* [NM_003193.5] (Arabi et al. 2011). A recurrent 12-bp deletion in exon 3 of *TBCE* (c.155-166del12) is particularly common among patients from the Middle East (Parvari et al. 1998; Khayat et al. 2024).

Although both disorders individually affect multiple organ systems, their coexistence has not previously been reported. We describe the first genetically confirmed patient with concurrent *RIT1*-associated NS and *TBCE*-related SSS, resulting in a blended phenotype. Additional heterozygous *CYP21A2* and *POLG* carrier variants further illustrate the genetic complexity of this case.

METHODS

This case report describes a neonate with concurrent NS and SSS. Clinical, biochemical, radiological, and molecular data were obtained through medical record review. Whole-exome sequencing was performed at Kuwait Medical Genetic Centre (KMGC), and variants were interpreted according to the American College of Medical Genetics and Genomics/Association for Molecular Pathology (ACMG/AMP) guidelines.

CASE PRESENTATION

A male infant was delivered by cesarean section at 36 weeks' gestation to a healthy 22-year-old Gravida 2 Para 2 mother; the parents are non-consanguineous but belonged to the same tribe. They had one healthy older child, with no history of pregnancy loss or similarly affected relatives; and the family history is unremarkable except for a maternal uncle with an unspecified disability. Antenatal ultrasonography (US) revealed severe symmetrical IUGR, decreased umbilical artery end-diastolic flow, bilateral moderate pleural effusions, and right renal pelvic dilatation. At birth, the infant was apneic, bradycardic, and markedly edematous, consistent with non-immune hydrops fetalis, requiring 7 minutes of resuscitation, endotracheal intubation, and neonatal intensive care unit admission for mechanical ventilation. Birth weight (1935 g), length (42 cm), and head circumference (28.6 cm) were all below the 3rd percentile.

The infant exhibited distinctive craniofacial dysmorphism (Fig. 1a-d), including hypertelorism, down-slanting palpebral fissures, a receding frontal hairline with low posterior hairline, bilateral low-set posteriorly rotated ears with left-sided fleshy helices, and brachycephaly. Additional phenotypic features included a webbed neck, broad chest with inferior pectus excavatum, widely spaced nipples, bilateral single transverse palmar creases, and inferior displacement of the fourth toe of the left foot (Fig. 1e-i). The constellation of dysmorphic features raised an early clinical suspicion of NS.

Postnatally, the infant developed bilateral pneumothoraces and pleural effusions requiring needle decompression, thoracentesis, and high-frequency oscillatory ventilation. His respiratory course was complicated by severe bronchopulmonary dysplasia (BPD) necessitating prolonged mechanical ventilation. He subsequently developed recurrent aspiration pneumonia secondary to severe gastroesophageal reflux, confirmed on upper gastrointestinal contrast study (Supplementary Fig. S1), with persistent feeding intolerance requiring trophic enteral feeds, prolonged parenteral nutrition, proton pump inhibitors, and a prokinetic agent (domperidone). Fundoplication and gastrostomy were considered but deferred because of young age, low weight, and clinical instability.

Echocardiography demonstrated a 3–4 mm atrial septal defect (ASD) with an aneurysmal interatrial septum, a 2 mm muscular ventricular septal defect (VSD), a patent ductus arteriosus (PDA), mild tricuspid regurgitation, mild right ventricular hypertrophy, and pulmonary hypertension, without arrhythmias. Repeat echocardiography and CT angiography demonstrated an incomplete circumflex double aortic arch with ASD, VSD, and a small PDA, without airway compression or tracheomalacia. Genitourinary findings included left-sided cryptorchidism, left multicystic dysplastic kidney (MCDK) (Fig. 2), and right nephrocalcinosis. Renal and electrolyte results are provided in Supplementary Table S7.

Initial cranial US was unremarkable. Serial US demonstrated bilateral echogenic thalamic hemorrhages on day 10 (Fig. 3), with brain magnetic resonance imaging (MRI) on day 17 revealing partial corpus callosum dysgenesis and hypoxic-ischemic encephalopathy (HIE) secondary to perinatal hypoxia (Fig. 4). Neurological examination subsequently demonstrated normal tone, spontaneous movements, and age-appropriate reflexes. On day 75, the infant developed hypocalcemic seizures (ionized calcium 1.0 mmol/L), managed with intravenous calcium, phenobarbitone, and levetiracetam.

Endocrine evaluation revealed congenital hypothyroidism and persistent hypocalcemia secondary to hypoparathyroidism, for which levothyroxine, calcium supplementation, and active vitamin D (One-Alpha) were initiated. Metabolic evaluation also demonstrated transient hyperammonemia (332 μmol/L), hyperlactatemia (14 mmol/L), and elevated branched-chain amino acids and methionine, which resolved with supportive management. Subsequent serum amino acid and urine organic acid profiles were normal, excluding inborn errors of metabolism. Newborn screening results are provided in Supplementary Table S1, repeated metabolic investigations and plasma amino acid chromatography results are summarized in Supplementary Tables S2 and S3, and thyroid and parathyroid hormone results are presented in Supplementary Table S8.

The hematologic course was characterized by persistent thrombocytopenia and bone marrow (BM) suppression, which were accompanied by immature myeloid cells on peripheral blood smear; BM examination excluded malignancy. Initial complete blood count, peripheral blood smear, and bone marrow aspirate findings are provided in Supplementary Tables S4-S6. Multiple transfusions of packed red blood cells, platelets, and fresh frozen plasma were required. The infant subsequently developed recurrent culture-confirmed sepsis due to methicillin-sensitive *Staphylococcus aureus* (MSSA), *Staphylococcus epidermidis*, and ultimately multidrug-resistant *Escherichia coli* (ESBL/NDM), progressing to refractory septic shock and multiorgan failure (MOF).

Given the extensive multisystem involvement, comprehensive genetic evaluation was performed. Cytogenetic and molecular findings and flow cytometry results are provided in Supplementary Tables S9 and S10. Chromosomal analysis revealed a normal male karyotype (46, XY). Whole-exome sequencing identified a heterozygous pathogenic *RIT1* variant (c.284G > C, p.Gly95Ala) and a homozygous pathogenic *TBCE* variant (c.155_166del, p.Ser52_Gly55del), confirming concurrent NS and SSS. Additional heterozygous pathogenic *CYP21A2* variant (c.955C > T, p.Gln319Ter) and a likely pathogenic *POLG* variant (c.1156C > T, p.Arg386Cys) were identified and interpreted as carrier states (Table 1).

Management involved a multidisciplinary team comprising neonatology, pulmonology, cardiology, endocrinology, nephrology, gastroenterology, hematology, pediatric surgery, genetics, metabolic medicine, nutrition, physiotherapy, and occupational therapy. Genetic counseling regarding recurrence risk and future reproductive planning was provided. Despite comprehensive multidisciplinary care, the infant died at 142 days of life from refractory septic shock and MOF.

Table 1
Whole-exome sequencing findings confirming the dual molecular diagnosis of concurrent Noonan syndrome and Sanjad–Sakati syndrome, with incidental carrier variants

Gene (NM)	OMIM N° (MOI)	Chromosomal Location	Variant	Zygosity	Classification	Relation to Phenotype
RIT1 (NM_006912.6)	*609591 (AD)*	chr1:155874247 C > G	c.284G > C (p.Gly95Ala)	Heterozygous	Pathogenic	Causative (Noonan syndrome)
TBCE (NM_003193.5)	*604934 (AR)*	chr1:235564868 GGGAGCCACGAAGGGA> GGGA	c.155_166del (p.Ser52_Gly55del)	Apparent Homozygous	Pathogenic	Causative (Sanjad–Sakati syndrome)
CYP21A2 (NM_000500.7)	*613815 (AR)*	chr6:32008198 C > T	c.955C > T (p.Gln319Ter)	Heterozygous	Pathogenic	Incidental carrier (Congenital adrenal hyperplasia)
POLG (NM_002693.3)	*174763 (AR, AD)*	chr15:89871930 G > A	c.1156C > T (p.Arg386Cys)	Heterozygous	Likely Pathogenic	Incidental carrier (POLG-related mitochondrial disease)
Reference transcripts: RIT1, NM_006912.6; *TBCE*, NM_003193.5*; CYP21A2*, NM_000500.7*; POLG*, NM_002693.3						

DISCUSSION

This case represents the first genetically confirmed coexistence of NS and SSS, in which concurrent pathogenic *RIT1* and *TBCE* variants resulted in a blended phenotype with extensive multisystem involvement. Prenatal findings of severe symmetrical IUGR, pleural effusions, and non-immune hydrops fetalis, together with postnatal craniofacial dysmorphism, webbed neck, CHD, renal anomaly, and thrombocytopenia, initially supported the diagnosis of severe neonatal NS, particularly the *RIT1*-associated phenotype. However, the subsequent development of congenital hypoparathyroidism, persistent hypocalcemia, congenital hypothyroidism, nephrocalcinosis, and severe feeding difficulties was more consistent with SSS caused by pathogenic *TBCE* variants. Additional heterozygous *CYP21A2* and *POLG* variants were identified and interpreted as incidental carrier states without phenotypic contribution.

Although the parents were non-consanguineous, they belonged to the same tribe. A recent meta-analysis reported greater genetic differentiation and higher homozygosity among tribal populations than other population groups (Rehman and Abbas 2025). Our case presented perinatally with severe symmetrical IUGR, pleural effusion, and non-immune hydrops fetalis. The latter two are recognized manifestations of NS secondary to lymphatic dysplasia, which occurs in fewer than 20% of cases and may result in pulmonary lymphangiectasia (Carcavilla et al. 2020). In contrast, severe growth restriction is a characteristic, albeit nonspecific, feature of SSS (Albaramki et al. 2012; David et al. 2021).

Our infant exhibited several characteristic craniofacial features of NS, including hypertelorism, down-slanting palpebral fissures, low-set posteriorly rotated ears with fleshy helices, and a low posterior hairline, all of which are among the most frequently reported features in the literature (Roberts 1993; Sharma et al. 2025). On the other hand, the characteristic craniofacial features of SSS, including microcephaly, a long narrow face, micrognathia, a beaked nose, deep-set eyes, thin lips, and large floppy ears, were absent (Elhassanien and Alghiaty 2013; Benchaib et al. 2024). Additional findings, including a webbed neck, broad chest with inferior pectus excavatum, and widely spaced nipples, further supported the diagnosis of NS (Allanson 1987; Carcavilla et al. 2020). Interestingly, bilateral single transverse palmar creases and inferior displacement of the left fourth toe have not been reported in association with either NS or SSS, potentially expanding the phenotypic spectrum of this dual genetic diagnosis.

Our patient developed severe gastroesophageal reflux with recurrent aspiration pneumonia and persistent feeding intolerance, consistent with the neonatal feeding difficulties reported in both NS (Carcavilla et al. 2020) and SSS (Arabi et al. 2011). CHD is a hallmark of NS (Carcavilla et al. 2020) but not typically associated with SSS. He exhibited characteristic cardiac anomalies of NS, including ASD, VSD, and ventricular hypertrophy (Roberts 1993; Roberts et al. 2013; Carcavilla et al. 2020), with additional cardiovascular findings, including an aneurysmal interatrial septum, PDA, tricuspid regurgitation, and an incomplete double aortic arch. Cryptorchidism, another common manifestation of NS, was also present (Carcavilla et al. 2020). The infant also manifested unilateral MCDK and contralateral nephrocalcinosis. While renal anomalies occur in approximately 10% of NS cases (Carcavilla et al. 2020), nephrocalcinosis has been reported in SSS secondary to hyperphosphatemia-related soft tissue and organ calcifications. (Elhassanien and Alghiaty 2013; Alghamdi 2022; Benchaib et al. 2024).

Persistent hypocalcemia secondary to hypoparathyroidism manifested as a hypocalcemic seizure at 75 days of age, consistent with the classical symptomatic hypocalcemia that typically manifests in SSS during infancy (Elhassanien and Alghiaty 2013; Benchaib et al. 2024). Congenital hypothyroidism was also present, in keeping with reports that approximately one-third of SSS cases exhibit either congenital or autoimmune thyroid dysfunction (David et al. 2021). Bilateral thalamic hemorrhages, corpus callosum dysgenesis, and HIE were accompanied by transient hyperammonemia, hyperlactatemia, and elevated branched-chain amino acids and methionine, all of which resolved with supportive management, excluding inborn errors of metabolism. In the literature, hypoparathyroidism-related metabolic disturbances in SSS have been associated with intracranial calcifications, corpus callosum anomalies, and rarely intracranial hemorrhage (Elhassanien and Alghiaty 2013). NS and related RASopathies are associated primarily with white matter and corpus callosum abnormalities, whereas thalamic hemorrhages are uncommon (Ayaz et al. 2023). Although NS is not typically associated with primary metabolic derangements, transient metabolic abnormalities have been reported in isolated pediatric cases (Zenker 2022). Collectively, these findings suggest that the neurological phenotype likely reflected the combined effects of the dual genetic diagnosis, severe systemic illness, and transient metabolic disturbances rather than a persistent metabolic disorder.

Our infant developed recurrent culture-confirmed sepsis caused by methicillin-sensitive *Staphylococcus aureus* (MSSA), *Staphylococcus epidermidis*, and ultimately multidrug-resistant *Escherichia coli* (ESBL/NDM), progressing to refractory septic shock

and MOF despite appropriate antimicrobial therapy. This clinical course aligns with SSS, in which infants are particularly susceptible to severe infections due to immune dysfunction, metabolic instability, poor nutritional status, and prolonged hospitalization (Elhassanien and Alghiaty 2013; Bashar et al. 2020). Although NS is not typically associated with primary immunodeficiency, increased susceptibility to infections has also been described in infants with NS and related RASopathies, potentially linked to lymphatic abnormalities and neonatal systemic stress (Smpokou et al. 2012). Our infant also exhibited persistent thrombocytopenia and BM suppression with immature myeloid cells, requiring repeated blood product transfusions. Although hematologic abnormalities are not characteristic of SSS, cytopenias and BM suppression have been reported in the context of severe systemic illness, metabolic disturbances, or sepsis (Elhassanien and Alghiaty 2013; Bashar et al. 2020). In contrast, NS is more commonly associated with hematologic manifestations, including thrombocytopenia, platelet function defects, and myeloproliferative disorders, particularly during infancy (Smpokou et al. 2012). Thus, the hematologic profile likely reflected both the underlying NS and the effects of critical illness.

Whole-exome sequencing established the dual diagnosis by identifying a heterozygous pathogenic *RIT1* variant (c.284G > C, p.Gly95Ala) and a homozygous pathogenic *TBCE* deletion (c.155_166del, p.Ser52_Gly55del), explaining the blended phenotype. Heterozygous activating *RIT1* variants are well-established causes of NS and are particularly associated with severe neonatal phenotypes, including lymphatic abnormalities and perinatal complications (Smpokou et al. 2012). Likewise, biallelic pathogenic *TBCE* variants are the molecular basis of SSS, particularly in patients of Middle Eastern descent (Elhassanien and Alghiaty 2013; Bashar et al. 2020). Additional heterozygous pathogenic *CYP21A2* variant (c.955C > T, p.Gln319Ter) and heterozygous likely pathogenic *POLG* variant (c.1156C > T, p.Arg386Cys), associated with AR congenital adrenal hyperplasia and *POLG*-related mitochondrial disorders, respectively (Cohen et al. 1993; Guarnotta et al. 2020; Silva et al. 2022), were both identified and interpreted as incidental carrier states without phenotypic contribution.

Despite comprehensive supportive care, the infant developed refractory septic shock and MOF. The prognosis of NS depends largely on the severity of cardiac and lymphatic involvement, with infants affected by CHD, BPD, or renal anomalies at increased risk of early mortality(Zenker 2022; Sharma et al. 2025). Similarly, SSS is associated with severe infections and poor clinical outcomes due to metabolic instability, immunologic compromise, and multisystem involvement (Benchaib et al. 2024). Management of SSS focuses on prompt correction of hypocalcemia with intravenous calcium infusion (Benchaib et al. 2024), followed by maintenance oral calcium and calcitriol (vitamin D) (Elhassanien and Alghiaty 2013; Benchaib et al. 2024), together with serum phosphate monitoring to prevent ectopic multiorgan calcifications (Albaramki et al. 2012). The coexistence of pathogenic *RIT1* and *TBCE* variants likely contributed to the exceptional severity and complexity of the clinical phenotype. This report expands the literature on neonatal NS and SSS, highlights the diagnostic challenges of blended phenotypes resulting from dual molecular diagnoses, and underscores the importance of early comprehensive genomic evaluation, multidisciplinary management, and genetic counseling in critically ill neonates with unexplained multisystem disease.

CONCLUSIONS

We report the first genetically confirmed coexistence of *RIT1*-associated NS and *TBCE*-related SSS, resulting in an exceptionally severe and complex clinical phenotype. This case demonstrates how blended genetic diagnoses can obscure clinical recognition and emphasizes the limitations of phenotype-based diagnosis in critically ill neonates. Whole-exome sequencing was essential for establishing the dual molecular diagnosis and guiding the subsequent management. Early genomic evaluation should be considered in neonates with unexplained multisystem disease, as timely molecular diagnosis facilitates prognostication, multidisciplinary care, and appropriate genetic counseling.

Declarations

Funding

This study received no specific funding.

Competing Interests

The authors declare no relevant financial or non-financial interests to disclose.

Ethical Approval

This case report was conducted in accordance with the ethical principles of the Declaration of Helsinki. Ethical approval for publication was obtained from the Institutional Review Board of the Kuwait Ministry of Health and Kuwait KMGC.

Consent to Publish

Written informed consent was obtained from the patient's parents for publication of anonymized clinical, molecular, and photographic data. Clinical photographs were anonymized by concealing the ocular regions to protect patient identity.

Data Availability Statement

The data supporting the findings of this case report are available from the corresponding author upon reasonable request. All shared data will be de-identified to protect patient confidentiality.

Author Contributions

M.Ab. collected the clinical data, documented the dysmorphic photographs, conducted the literature review, drafted the initial manuscript, and finalized the manuscript. M.Ay supervised the project, provided substantial intellectual input, and critically reviewed and revised the manuscript. A.R., D.I., and Y.F. provided comprehensive clinical evaluations and multidisciplinary management of the patient. M.Ay., D.I., and L.B. provided expert clinical input and critically reviewed and revised the manuscript. All authors read and approved the final manuscript.

References

1. Albaramki J, Akl K, Al-Muhtaseb A, et al. Sanjad Sakati syndrome: a case series from Jordan. East Mediterr Health J. 2012;18:527–31. https://doi.org/10.26719/2012.18.5.527.
2. Alghamdi S. Oral Facial Manifestations of Sanjad–Sakati Syndrome: A Literature Review. Children. 2022;9:448. https://doi.org/10.3390/children9040448.
3. Allanson JE. Noonan syndrome. J Med Genet. 1987;24:9–13. https://doi.org/10.1136/jmg.24.1.9.
4. Aoki Y, Niihori T, Banjo T, et al. Gain-of-function mutations in RIT1 cause Noonan syndrome, a RAS/MAPK pathway syndrome. Am J Hum Genet. 2013;93:173–80. https://doi.org/10.1016/j.ajhg.2013.05.021.
5. Aoki Y, Niihori T, Inoue S, Matsubara Y. Recent advances in RASopathies. J Hum Genet. 2016;61:33–9. https://doi.org/10.1038/jhg.2015.114.
6. Arabi WA, Basheer AA, Abdullah MA. Sanjad-Sakati Syndrome in Sudanese children. Sudan J Paediatr. 2011;11:42–7.
7. Ayaz E, Yıldırım R, Çelebi C, Ozalkak S. Noonan syndrome: Neuroimaging findings and morphometric analysis of the cranium base and posterior fossa in children. J Neuroimaging. 2023;33:318–27. https://doi.org/10.1111/jon.13075.
8. Bashar M, Taimur M, Amreek F et al. (2020) Endocrinological Manifestations of Sanjad-Sakati Syndrome. Cureus. https://doi.org/10.7759/cureus.8770
9. Benchaib NEH, Elouali A, Sara A, Cureus et al. https://doi.org/10.7759/cureus.66429
10. Carcavilla A, Suárez-Ortega L, Sánchez AR, et al. Noonan syndrome: genetic and clinical update and treatment options. Anales de Pediatría (English Edition). 2020;93. https://doi.org/10.1016/j.anpede.2020.04.009. :61.e1-61.e14.
11. Cohen BH, Chinnery PF, Copeland WC. (1993) POLG-Related Disorders.
12. David O, Barash G, Agur R, et al. Multiple Endocrine Deficiencies are Common in Hypoparathyroidism–Retardation–Dysmorphism Syndrome. J Clin Endocrinol Metab. 2021;106:e907–16. https://doi.org/10.1210/clinem/dgaa807.
13. Elhassanien AF, Alghiaty. Neurological manifestations in children with Sanjad-Sakati syndrome. Int J Gen Med 393. 2013. https://doi.org/10.2147/IJGM.S40930.
14. Guarnotta V, Niceta M, Bono M, et al. Clinical and hormonal characteristics in heterozygote carriers of congenital adrenal hyperplasia. J Steroid Biochem Mol Biol. 2020;198:105554. https://doi.org/10.1016/j.jsbmb.2019.105554.
15. Khayat AM, Alshareef BG, Alharbi SF, et al. Consanguineous Marriage and Its Association With Genetic Disorders in Saudi Arabia: A Review. Cureus. 2024;16:e53888. https://doi.org/10.7759/cureus.53888.

16. Parvari R, Hershkovitz E, Kanis A, et al. Homozygosity and Linkage-Disequilibrium Mapping of the Syndrome of Congenital Hypoparathyroidism, Growth and Mental Retardation, and Dysmorphism to a 1-cM Interval on Chromosome 1q42-43. Am J Hum Genet. 1998;63:163–9. https://doi.org/10.1086/301915.
17. Rehman SU, Abbas GH. Human genetic diversity across South Asian populations: A systematic review and meta-analysis. Medicine. 2025;104:e44147. https://doi.org/10.1097/MD.0000000000044147.
18. Roberts AE. (1993) Noonan Syndrome.
19. Roberts AE, Allanson JE, Tartaglia M, Gelb BD. Noonan syndrome. Lancet. 2013;381:333–42. https://doi.org/10.1016/S0140-6736(12)61023-X.
20. Saint-Laurent C, Mazeyrie L, Yart A, Edouard T. Novel therapeutic perspectives in Noonan syndrome and RASopathies. Eur J Pediatr. 2023;183:1011–9. https://doi.org/10.1007/s00431-023-05263-y.
21. Sharma L, Winters R, Morales A. (2025) Noonan Syndrome.
22. Silva RS, Carvalho B, Pedro J, et al. Differences in hormonal levels between heterozygous CYP21A2 pathogenic variant carriers, non-carriers, and females with non-classic congenital hyperplasia. Arch Endocrinol Metab. 2022. https://doi.org/10.20945/2359-3997000000437.
23. Smpokou P, Tworog-Dube E, Kucherlapati RS, Roberts AE. Medical complications, clinical findings, and educational outcomes in adults with Noonan syndrome. Am J Med Genet A. 2012;158A:3106–11. https://doi.org/10.1002/ajmg.a.35639.
24. Zenker M. Clinical overview RASopathies. Am J Med Genet C Semin Med Genet. 2022;190:414–24. https://doi.org/10.1002/ajmg.c.32015.
25. Zenker M, Edouard T, Blair JC, Cappa M. Noonan syndrome: improving recognition and diagnosis. Arch Dis Child. 2022;107:1073–8. https://doi.org/10.1136/archdischild-2021-322858.

Figures

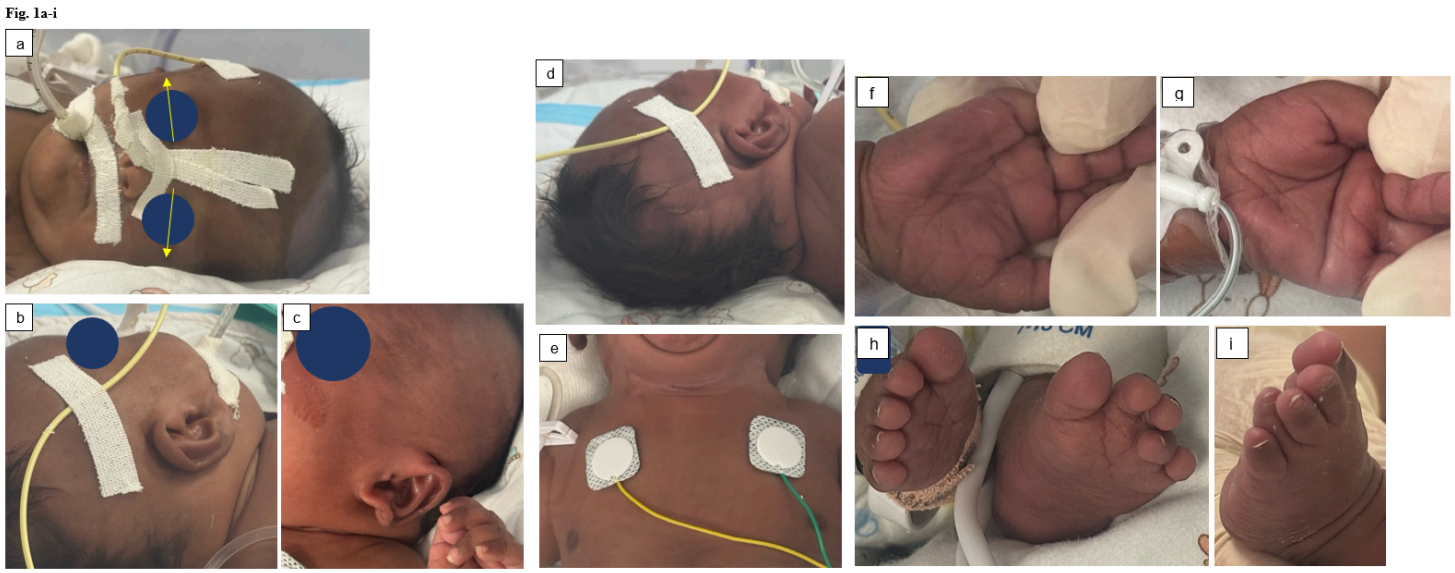


Figure 1

Clinical photographs demonstrating dysmorphic features. **a** Hypertelorism and down-slanting palpebral fissures. **b, c**Lateral facial views demonstrating low-set posteriorly rotated ears with fleshy helices. **d** Receding frontal hairline and low posterior hairline. **e** Webbed neck, broad chest with widely spaced nipples, and inferior pectus excavatum. **f, g** Bilateral single transverse palmar creases. **h, i** Inferior displacement of the fourth toe of the left foot

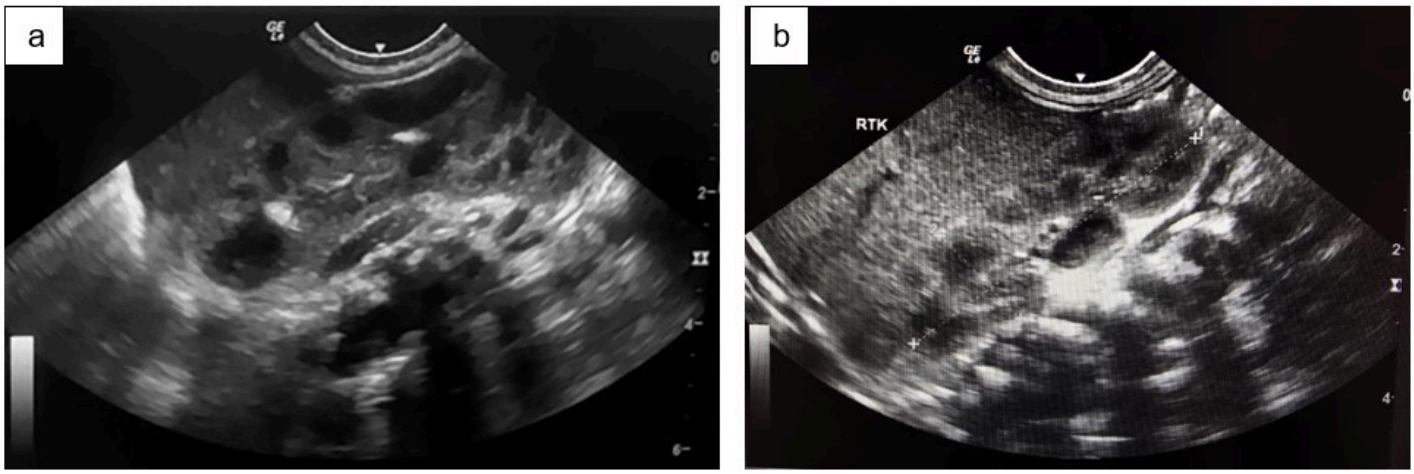


Figure 2

Renal ultrasonography. **a** Left multicystic dysplastic kidney (MCDK). **b** Right nephrocalcinosis

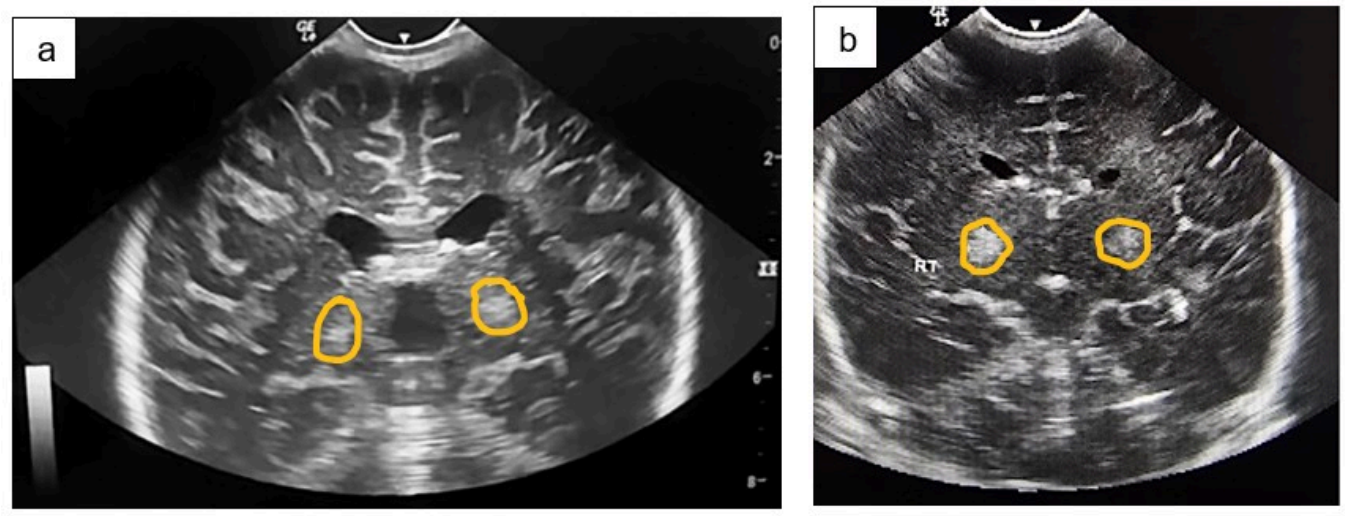


Figure 3

Cranial ultrasonography. **a, b** Bilateral hyperechoic thalamic lesions consistent with bilateral thalamic hemorrhages

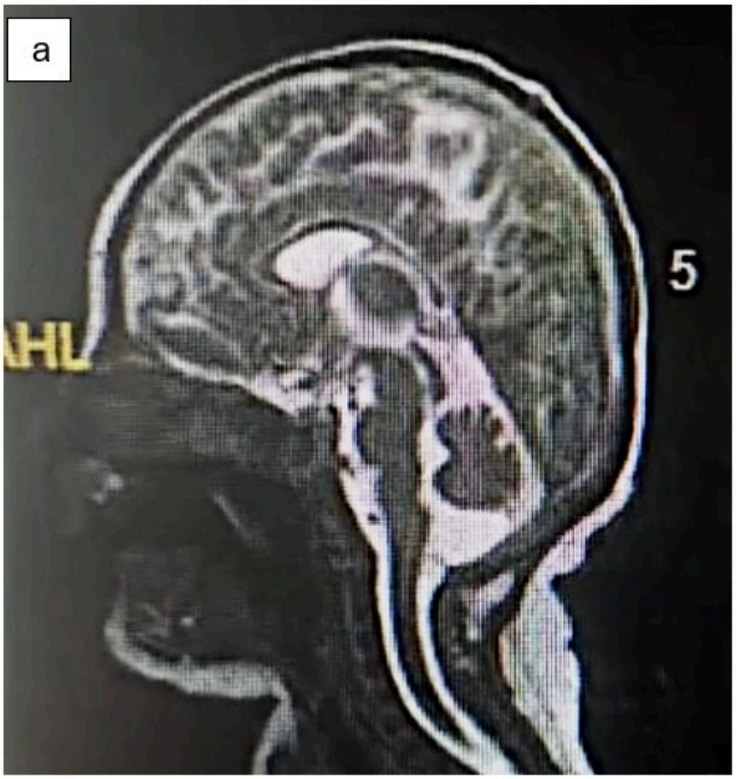


Figure 4

Mid-sagittal brain magnetic resonance image demonstrating hypoplasia of the splenium with relative preservation of the genu, consistent with partial corpus callosum dysgenesis

Supplementary Files

This is a list of supplementary files associated with this preprint. Click to download.

- NSSSSSupplementary.pdf